Supplementary Information

Reduced graphene oxides prepared via non-explosive thermal reduction for supercapacitors with high volumetric capacitance

Jianing Tan[1], Zhaoyuan Liu[1,2] *, Wei Wu[1], Gang Li[1], Wei Guo[1,2] *

[a]*School of Chemistry and Chemical Engineering, Harbin Normal University, Harbin 150025, P. R. China. E-mail: lzy@hrbnu.edu.cn, guowei@hrbnu.edu.cn*

[b]*State Key Laboratory of Photochemical Biomaterials and Energy Storage Materials, Harbin Normal University, Harbin 150025, P. R. China.*

†Electronic supplementary information (ESI) available.

1. Supplementary methods

1.1 Supplementary characterization

The microsturcture and morphology of the samples were examined by scanning electron microscopy (SEM, Helios Nanolab 600i) and high-resolution transmission electron microscopy (HR-TEM, FEI Tecnai G2 F30). The X-ray photoelectron spectroscopy (XPS) was executed on a Thermo Fisher spectrometer with an Al Kα (*hv*=1486.69 eV) X-ray source. The spectra were fitted using the sum form of Gaussian and Lorentzian function (75% Gaussian and 25% Lorentzian characters) and the Shirley background. The Fourier Transform Infrared (FTIR) spectra were recorded in KBr pellets using an IR Tracer 100 in the wavenumber region 4000 to 400 cm^{-1}. The powder X-ray diffraction (XRD) measurements were carried out on a Rigaku Ultima IV with Cu Kα irradiation (λ=1.54 Å). The Raman spectra were recorded using a B&WTEK spectrometer (BWS435-532SY) with a 523 nm laser (*hv*=2.34 eV), 10% laser power (total power: 240 mW). The nitrogen adsorption/desorption isotherms were measured using a Micromeritics ASAP 2020 HD88. The specific surface area and pore size distribution were determined by Brunauer-Emmett-Teller (BET) [1] and Barrett-Joyner-Halenda (BJH) desorption analyses, respectively. The packing density ρ of RGOs was calculated through the following equation:

$$\rho_m = (V_{total} + 1/\rho_{carbon})^{-1} \quad (1)$$

where ρ_m is the particle density of the materials and the ρ_{carbon} is the true density of carbon (2 g cm^{-3}), V_{total} is the total pore volume estimated from N_2 isotherm at 77 K. Thermogravimetric analysis (TG) and Differential scanning calorimetry (DSC) measurements were performed on a Perkin Elmer instrument (Diamond 6300) and STA449F5 (Netzsch, Germany), respectively. It is heated from room temperature to 600 ℃ at a rate of 10 ℃ min^{-1} in an inert atmosphere.

1.2 Supplementary electrochemical measurements

The working electrode was fabricated by blending the active materials, polyvinylidene fluoride (PVDF), and acetylene black in a weight ratio of 8:1:1 using N-methyl-2-pyrrolidone (NMP) as the solvent until a consistent slurry was formed. The as-prepared slurry was dropped onto the stainless-steel mesh (300 mesh) with areal of 1 cm^2. The electrode was dried at 120 °C in a vacuum oven for 12 h. Then, the electrode was pressed at 10 MPa for 10 minutes to enhance the packing density. The mass loading of the active materials on the electrode is regulated through controlling the slurry volume deposited on the stainless-steel mesh. The prepared electrode, Ag/AgCl ($KCl_{sat.}$) electrode and a slice of platinum served as working, reference and counter electrodes, respectively. The cyclic voltammetry (CV) tests were investigated between -0.2 and 1.0 V (vs. Ag/AgCl). The galvanostatic charge/discharge (GCD) was performed in the same potential range at the current densities ranging from 0.1 to 100 A g^{-1}. The electrochemical impendence spectroscopy (EIS) measurements were evaluated in the frequency range from 100 kHz to 0.01 Hz at open circuit potential with an ac perturbation of 5 mV. The simulation of the experiment impedance using three-electrode data was carried out with Zview software.

Calculation of the specific capacitances:

(1) Three-electrode configuration

The gravimetric specific capacitances based on the active material (C_g, F g^{-1}) were calculated according to the curves of constant current charge/discharge at different current densities:

$$C_g = \frac{I\Delta t}{m\Delta U} \tag{2}$$

where I is the discharge current (A), Δt is the discharge time (s), m is the weight of the active material (g), and ΔU is the discharge voltage (V) excluding the internal resistance

(iR) drop during the discharge process.

The volumetric performances of the active materials (C_V, F cm^{-3}) were calculated according to the following equation:

$$C_v = C_g \times \rho_m \tag{3}$$

where C_g presents the gravimetric capacitance of the active material, ρ_m is the packing density (g cm^{-3}) of the active material.

The areal specific capacitance (C_A, F cm^{-2}) was calculated according to the following equation:

$$C_A = C_g \times \rho_A \tag{4}$$

where C_A (mF cm^{-2}) is the geometric areal specific capacitance and ρ_A (mg cm^{-2}) is the mass loading of active materials.

(2) Two-electrode configuration

The gravimetric specific capacitance of the device was calculated by the following equation:

$$C_{g\text{-}2e} = \frac{I\Delta t}{2m\Delta U} \tag{5}$$

where I is the discharge current (A), Δt is the discharge time (s), m is the weight of the active material in the individual electrode (g), and ΔU is the discharge voltage (V) excluding the iR drop during the discharge process.

The energy densities (E) and power density (P) of the symmetric cell were estimated according to the following equation:

$$E = \frac{1}{2} C \times \Delta U^2 \tag{6}$$

$$P = \frac{E}{t} \tag{7}$$

Where C represents the gravimetric/areal/volumetric capacitance based on the two-

electrode system. ΔU is the discharge voltage excluding the iR drop during the discharge process, and t is the discharging time measured in the galvanostatic charging and discharging experiments.

2. Supplementary Figures and Tables

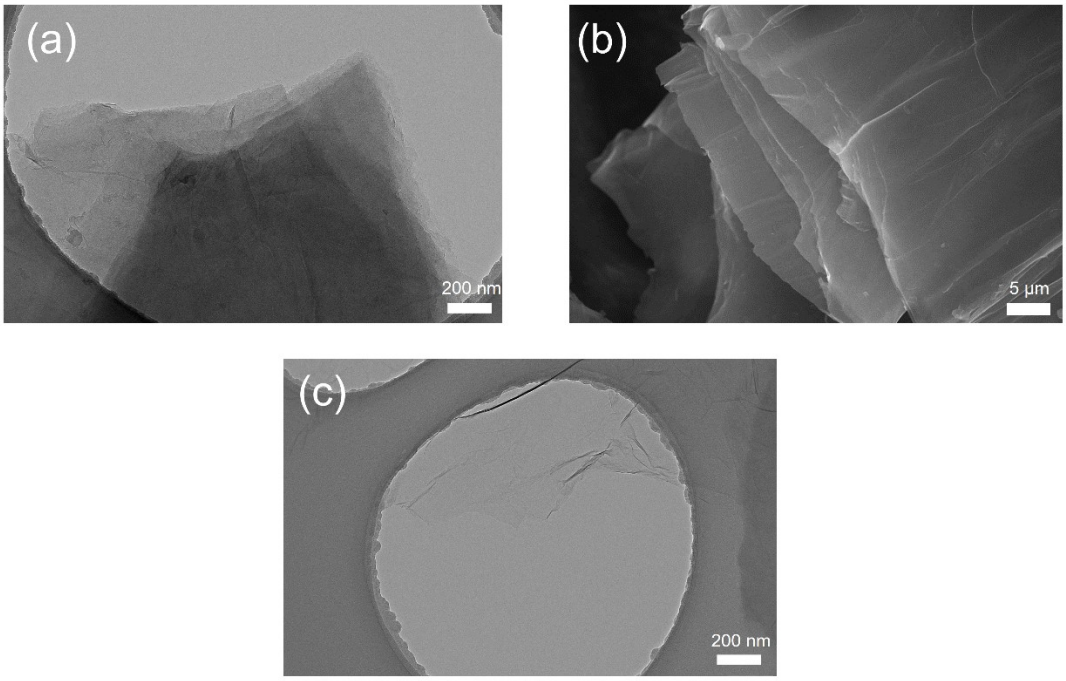

Fig. S1 (a) The TEM images of RGO-300-1.35. (b) The SEM images of GO-1.35. (c) The TEM images of RGO-300-6.02.

Fig. S2 The optical photograph of (a) GO-6.02 and (b) RGO-300-6.02.

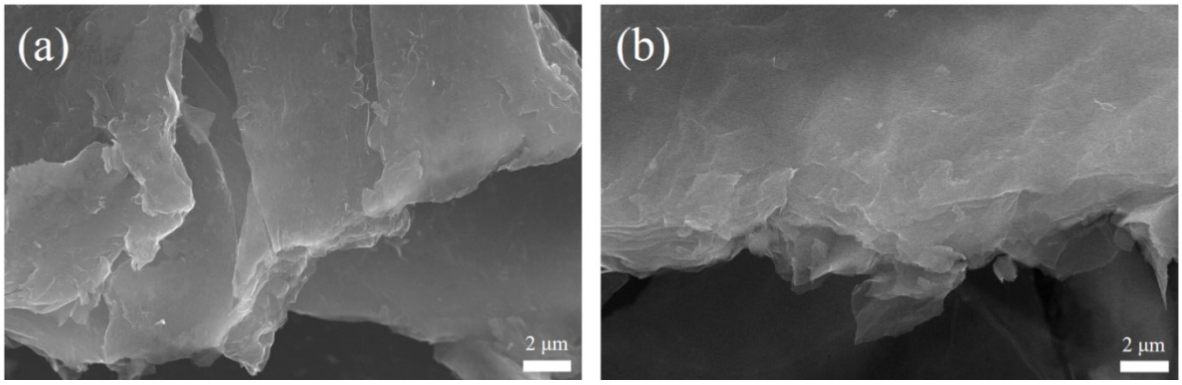

Fig. S3 The SEM images of (a) RGO-200-1.35. (b) RGO-400-1.35.

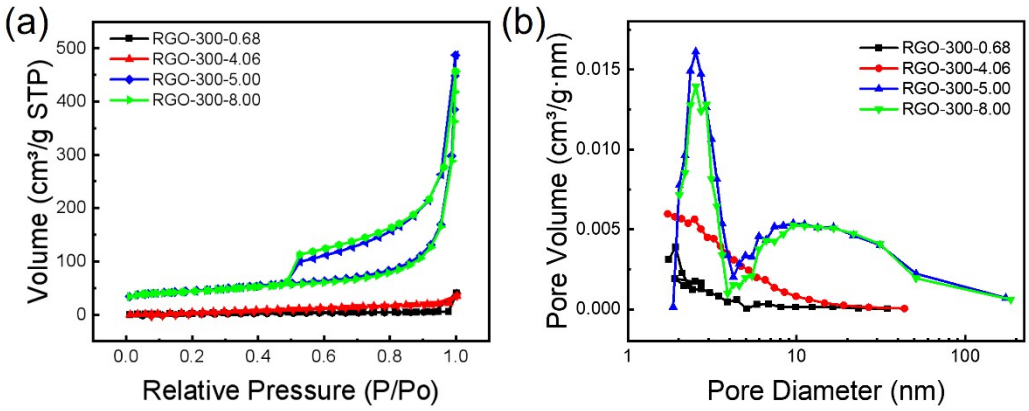

Fig. S4 (a) Nitrogen adsorption/desorption isotherms and (b) pore size distribution curves of RGO-300-0.68, RGO-300-4.06, RGO-300-5.00 and RGO-300-8.00.

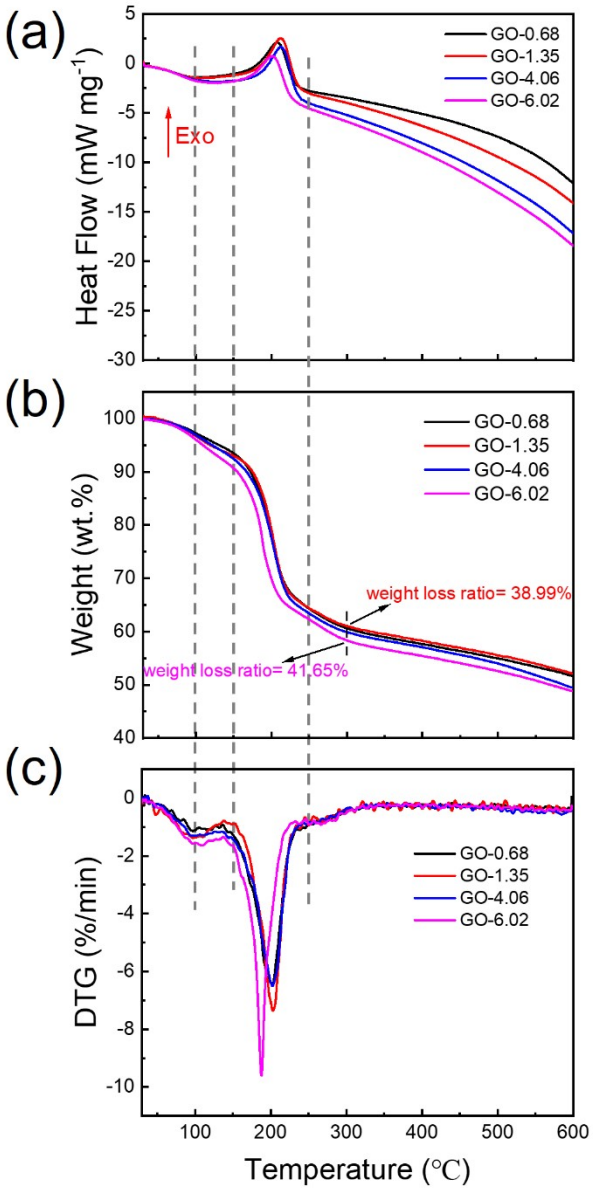

Fig. S5 (a) TGA, (b) DSC and (c) DTG curves for GO films with different mass loadings.

TGA curves of all the GO samples show three major weight loss stages. The first stage starting from room temperature to around 100 °C suffers a weight loss of about 5%, which is attributed to the removal of physically adsorbed or hydrated water. The second stage is in the range of 100–250 °C with a sharp weight loss of around 35% and an exothermic DSC peak. This is an acknowledged GO thermal reduction process, in which most oxygen-containing functional moieties are transformed into CO, CO_2 and

H_2O. The third stage weight loss at temperatures above 250 °C is related to the thermal decomposition of GO.

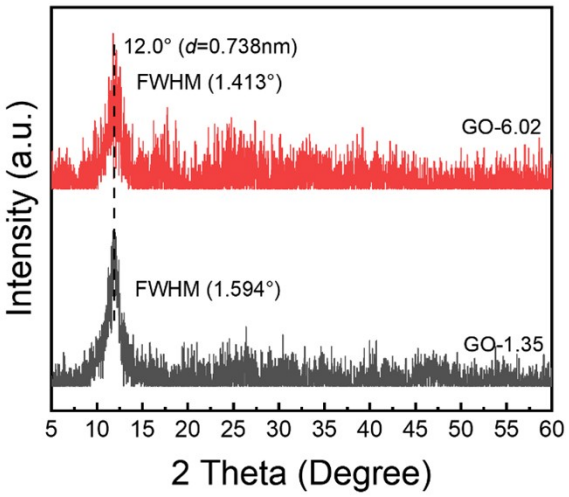

Fig. S6 XRD of GO-1.35 and GO-6.02.

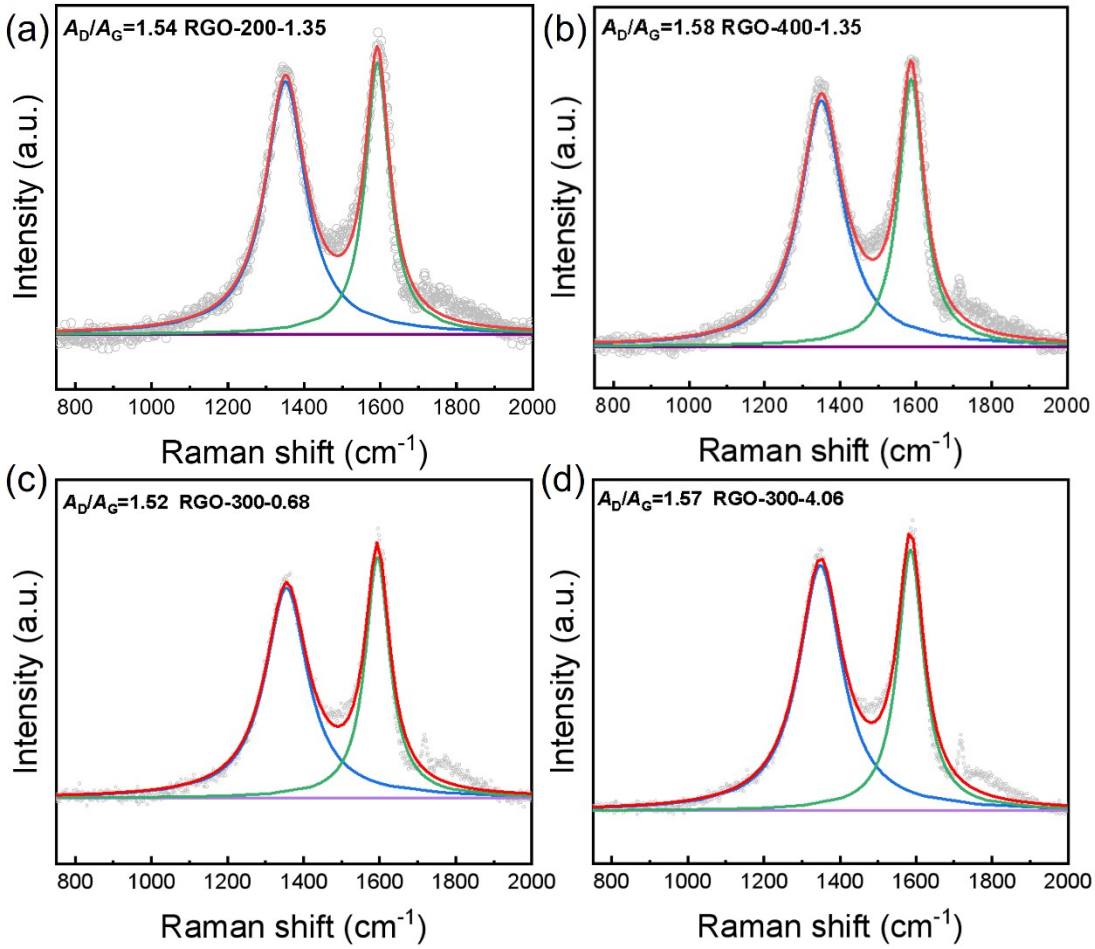

Fig. S7 Raman spectra of (a) RGO-200-1.35 (b) RGO-400-1.35 (c) RGO-300-0.68 and (d) RGO-300-4.06.

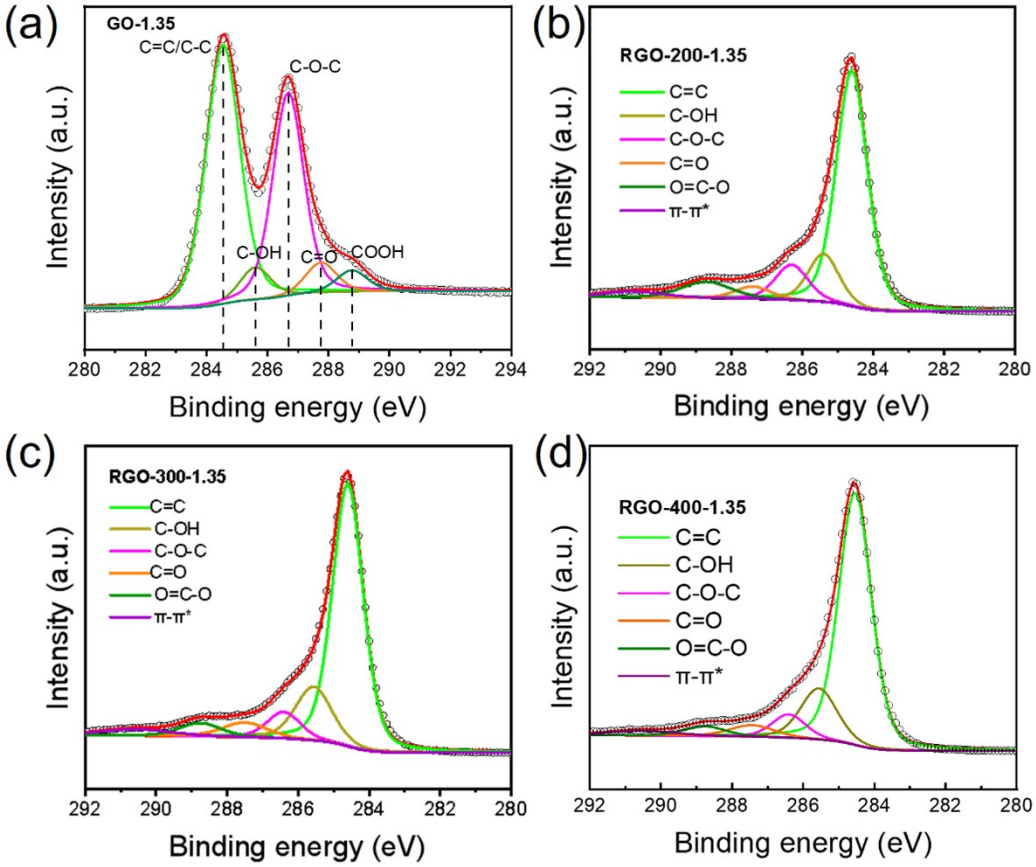

Fig. S8 High-resolution C1s spectra of (a) GO-1.35. (b) RGO-200-1.35. (c) RGO-300-1.35 and (d) RGO-400-1.35.

The high-resolution C 1s spectra can be deconvoluted into six peaks according to the reported literature [1, 2], as shown in Fig. S8. The components of C=C, C–OH, C–O–C, C=O, O=C-O and π–π* are located at 284.6 eV, 285.5 eV, 286.5 eV, 287.5 eV, 288.8 eV, and 290.6 eV, respectively.

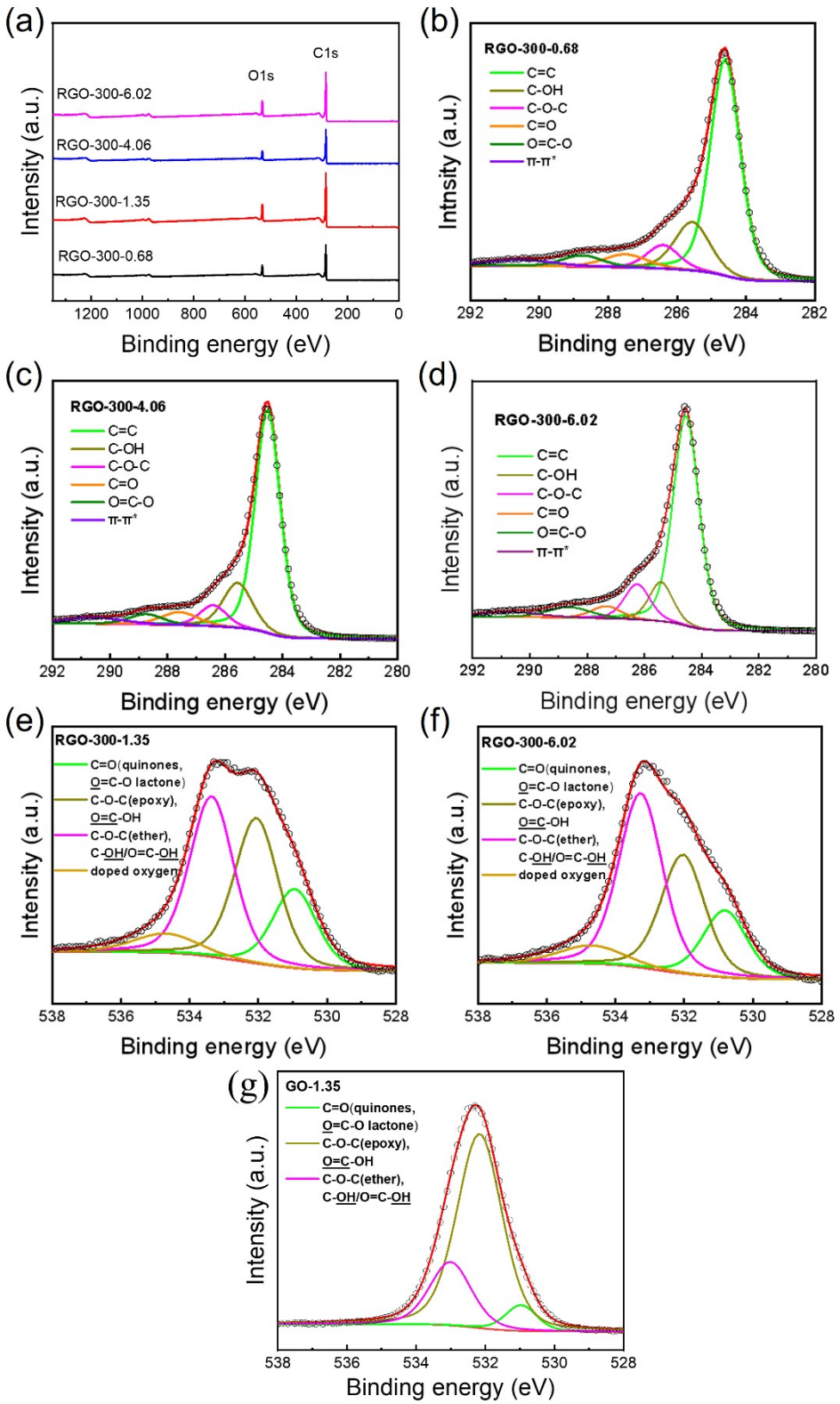

Fig. S9 (a) XPS survey spectra of RGO-300s. High-resolution C 1s spectra of (b) RGO-300-0.68, (c) RGO-300-4.06 and (d) RGO-300-6.02, High-resolution O 1s spectra of (e) RGO-300-1.35, (f) RGO-300-6.02 and (g) GO-1.35.

As shown in Figure S9e-S9g, the O 1s spectrum can be fitted with four peaks located at 530.3 eV, 531.5 eV, 533.1 eV, and 534.7 eV, corresponding to four types of oxygen [3-5]. The peak at 530.3eV corresponds to C=O of quinoid and lactone. The peak at 531.5 eV corresponds to C-O-C (epoxy) and C=O of carboxyl group. The peak at 533.1 eV corresponds to single-bonded oxygen such as C-O-C (ether), C-OH and O=C-OH. The peak at 534.7 eV corresponds to doped oxygen, which represents oxygen doped near or within the in-plane pores of graphene. The contents of O1, O2, and O3 in GO-1.35 are 6.6%, 71.8%, and 21.6%, respectively, indicating a relatively high proportion of epoxy groups in GO-1.35.

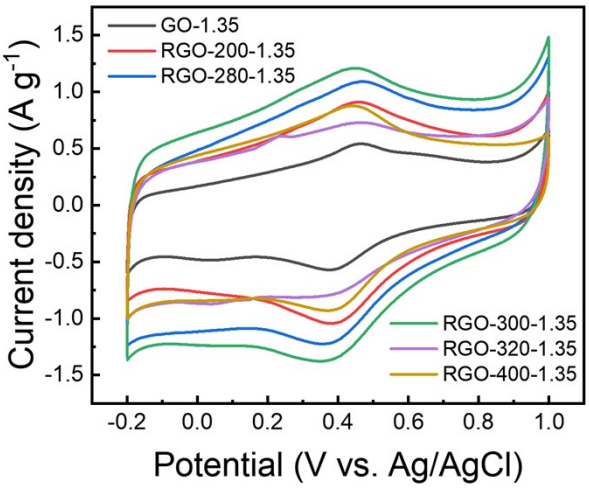

Fig. S10 CV curves comparison at 5 mV s^{-1}

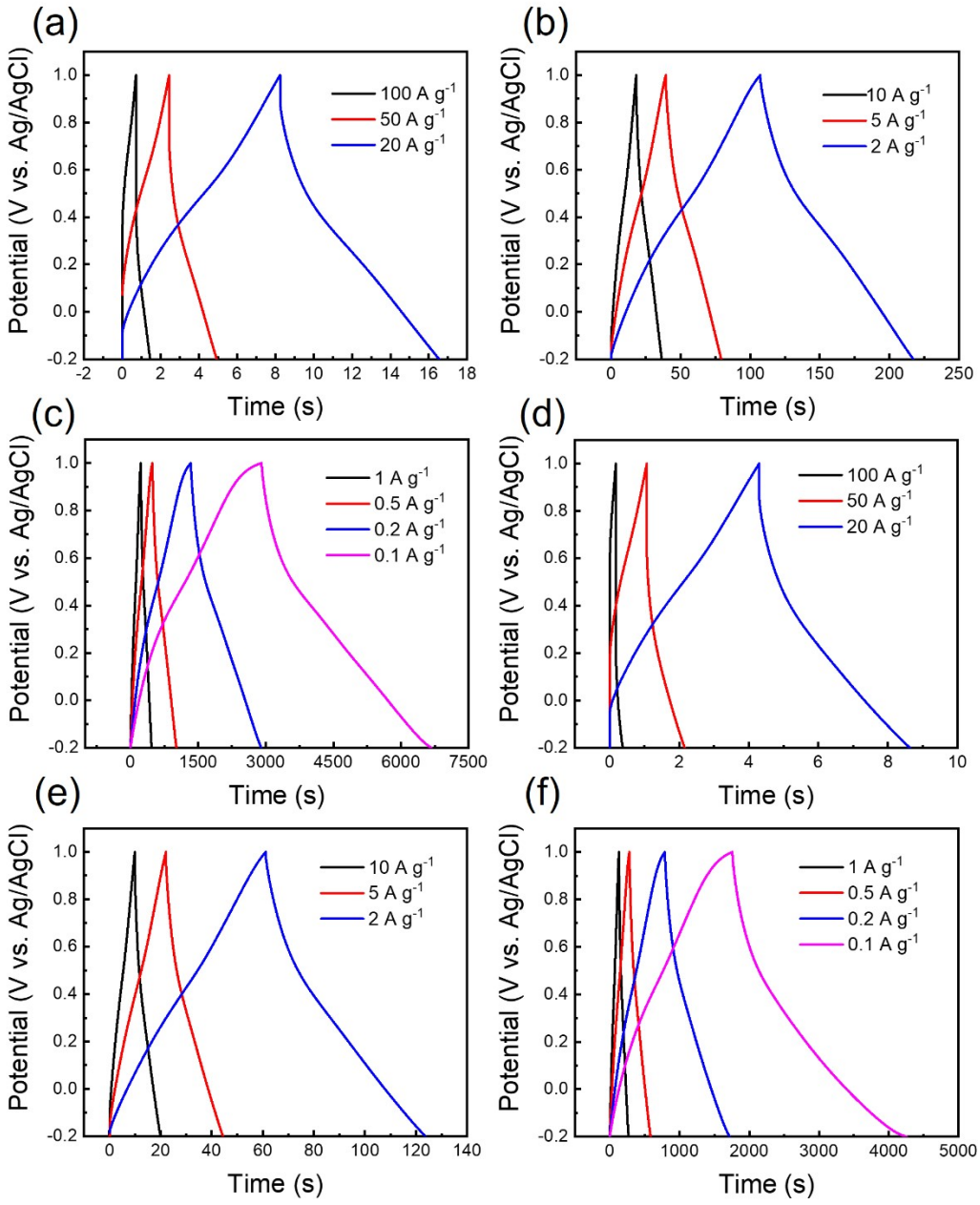

Fig. S11 (a)-(c) GCD curves of RGO-300-1.35 at different current densities. (d)-(f) GCD curves of RGO-300-6.02 at different current densities.

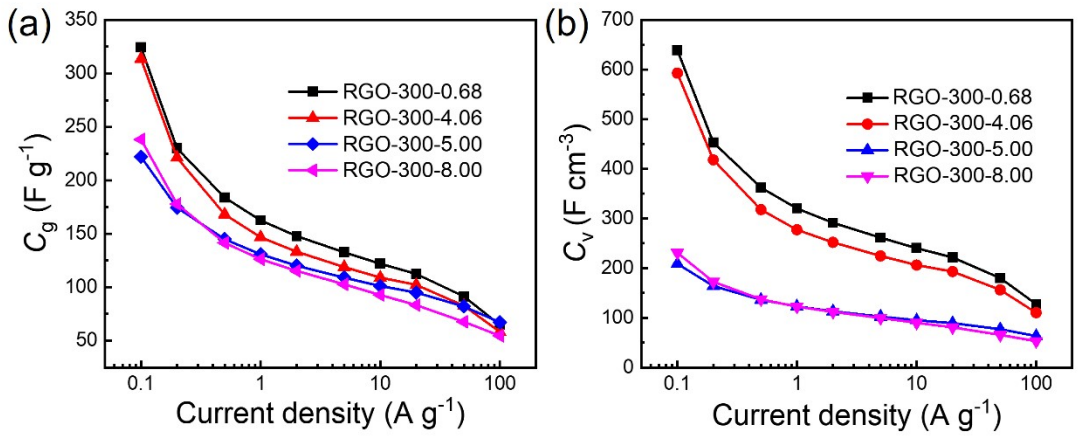

Fig. S12 (a) Comparison of gravimetric capacitance (C_g) and (b) volumetric capacitance (C_V) of RGO-300s at various current densities.

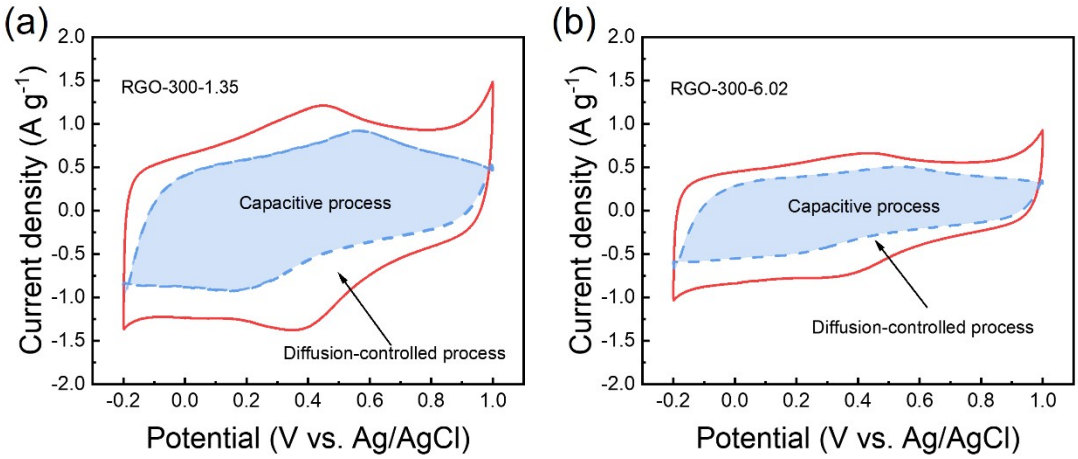

Fig. S13 The mechanism of charge storage. Decoupling of the total capacitance contributed by capacitive process and diffusion-controlled process of (a) RGO-300-1.35 and (b) RGO-300-6.02.

The shaded part surrounded by dotted lines is the capacitive current, and the total CV curve area minus the capacitive current is the current of the diffusion control part. The redox peaks are still present in the curves of capacitive charges, indicating that the redox process between C-OH and C=O is a surface redox reaction.

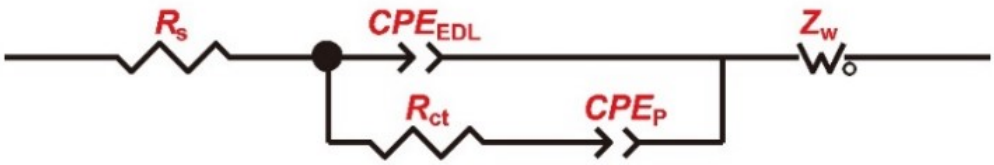

Fig. S14 The equivalent electric circuit model used for fitting the Nyquist plots. *R*s : the intrinsic ohmic resistance; *R*ct: charge transfer resistance; *CPE*EDL: constant phase element representing the electrical double layer capacitance (EDLC); *CPE*P: constant phase element representing the pseudocapacitance provided by the oxygen functional groups; Z_w: a Generalized Finite Warburg element terminating in an open circuit.

Table S1 The parameters of specific surface area (SSA), total pore volume and average pore size calculated from nitrogen absorption/adsorption isotherms. The packing density was calculated based on the equation (1).

Samples	BET SSA (m^2 g^{-1})	Total pore volume (cm^3 g^{-1})	Average Pore size (nm)	Packing density (g cm^{-3})
GO-1.35	9	0.0022	12	1.99
RGO-300-0.68	22	0.0064	4	1.97
RGO-300-1.35	9	0.017	5	1.94
RGO-300-4.06	56	0.03	5	1.89
RGO-300-5.00	154	0.56	24	0.94
RGO-300-6.02	177	0.62	17	0.89
RGO-300-8.00	151	0.53	24	0.97

Table S2 The peak temperature and peak area parameters were obtained by DSC testing.

Samples	Peak (℃)	Delta H (J/g)
GO-0.68	208.3	890.0
GO-1.35	213.0	1612.9
GO-4.06	213.2	1553.4
GO-6.02	201.9	1446.9

Table S3 OCFGs relative intensity ratios of RGO-300-1.35 and RGO-300-6.02 measured in FTIR.

Samples	$I_{C=O\ (1700)}/I_{C=C}$	$I_{C=O\ (1731)}/I_{C=C}$	$I_{C-OH}/I_{C=C}$
RGO-300-1.35	0.54	0.48	0.83
RGO-300-6.02	0.41	0.44	0.75

Table S4 The contents of functional groups estimated by the XPS area in the high-resolution C 1s peak. (Unit: %)

Samples	C=C	C-OH	C-O-C	C=O	O-C=O	π-π*
GO-1.35	49.7	5.6	35.6	5.3	3.8	0
RGO-200-1.35	64.3	15.1	6.7	5.1	5.1	3.7
RGO-300-1.35	64.4	15.5	7.0	5.2	4.4	3.5
RGO-400-1.35	67.9	15.3	6.4	4.3	3.3	2.7
RGO-300-0.68	62.4	16.5	7.3	5.5	4.4	4.0
RGO-300-4.06	64.7	15.3	6.5	5.4	4.0	4.1
RGO-300-6.02	65.3	14.4	7.7	5.2	3.5	3.9

Table S5 The contents of oxygen functional groups of RGO-300-1.35 and RGO-300-6.02 estimated by the XPS area in the high-resolution O 1s peak. (Unit: %).

Samples	C=O (quinones, O=C-O lactone)	C-O-C (epoxy), O=C-OH	C-O-C (ether), C-OH, O=C-OH	doped oxygen
GO-1.35	6.6	71.8	21.6	0
RGO-300-1.35	19.1	35.2	38.8	6.9
RGO-300-6.02	17.3	30.6	45.1	7.0

Table S6 The resistance values obtained from the fitting results. (Unit: Ohm)

Samples	R_{ct}	R_s
RGO-300-0.68	0.21	0.88
RGO-300-1.35	0.15	1.1
RGO-300-4.06	0.33	1.0
RGO-300-6.02	0.47	1.0

Supplementary references

1. W. Y. Fu L, Zhang K, Zhang W, Chen J, Deng Y, Du Y, Tang N, *ACS Nano*, 2019, **13**, 6341-6347.

2. A. Ganguly, S. Sharma, P. Papakonstantinou and J. Hamilton, *J. Phys. Chem. C*, 2011, **115**, 17009-17019.

3. Y. Lin, X. G. Han, C. J. Campbell, J. W. Kim, B. Zhao, W. Luo, J. Q. Dai, L. B. Hu and J. W. Connell, *Adv. Funct. Mater.*, 2015, **25**, 2920-2927.

4. Y. Yamada, H. Yasuda, K. Murota, M. Nakamura, T. Sodesawa and S. Sato, *J. Mater. Sci.*, 2013, **48**, 8171-8198.

5. R. Larciprete, P. Lacovig, S. Gardonio, A. Baraldi and S. Lizzit, *J. Phys. Chem. C*, 2012, **116**, 9900-9908.